RSC Advances

PAPER

Cite this: *RSC Adv.*, 2018, **8**, 31673

Design of nanostructured hybrid materials: twin polymerization of urethane-based twin prepolymers†

D. Uhlig,[a] S. Spange,[a] A. Seifert,[a] K. Nagel,[a] S. Anders,[b] L. Kroll,[b] R. Stoll,[c] F. Thielbeer,[d] P. Müller[d] and K. Schreiter*[a]

Received 21st June 2018
Accepted 4th September 2018

DOI: 10.1039/c8ra05310c

rsc.li/rsc-advances

Organic–inorganic hybrid materials with urethane functionalities were obtained by simultaneous twin polymerization of twin prepolymers in combination with the ideal twin monomer 2,2′-spirobi[4*H*-1,3,2-benzodioxasiline]. The twin prepolymers consist of a urethane-based prepolymer with reactive terminal groups which can react during the twin polymerization process. Nanostructured hybrid materials with integrated dialkylsiloxane crosslinked urethane structures, phenolic resin and SiO_2 are obtained in a one pot process. The effects of the polymerization temperature as well as those of various catalysts and reagent ratios on the polymerization behavior were investigated. The molecular structures of the obtained materials were determined by ^{13}C- and ^{29}Si-{^{1}H}-CP-MAS NMR spectroscopies. HAADF-STEM-measurements were performed to prove the distribution of silicon in the hybrid material.

Introduction

Nanostructured materials are one of the emerging areas of materials science and have attracted much attention because of their possible use in areas such as microelectronics, sensors, photovoltaics, electro-optical instruments, energy storage, conversion and separation processes as well as in catalysis.[1–9] In recent years a variety of methods for the preparation of organic–inorganic hybrid materials (HMs) have been developed which deliver defined nanostructures with domain sizes of 2 to 100 nm. In particular silica-based organic–inorganic HMs have been investigated since they combine the distinctive properties of organic polymers (*e.g.* malleability, good impact resistance, flexibility) and silica (*e.g.* high mechanical strength, transparency, good chemical and thermal stability) as well as some special or new types of properties based on their specific microstructure.[9]

The sol–gel procedure and template-assisted polymerization are the most frequently used methods for preparing silica-based organic–inorganic HMs both on the micro scale and at the molecular level.[10,11] However, most established synthetic methods require subsequent processing steps.

In recent years the twin polymerization (TP) turned out to be an elegant tool to prepare nanostructured HMs with domain sizes from 0.5 up to 10 nm whereby two different polymer phases result from only one single source monomer.[12–16] For instance, the polymerization of the "ideal" twin monomer 2,2′spirobi-[4*H*-1,3,2-benzodioxasiline] (**1**) leads to a HM consisting of phenolic resin and silica (Scheme 1a).[13,14] Different

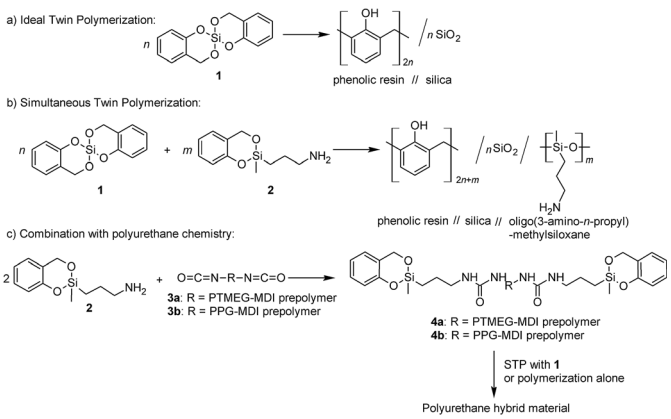

Scheme 1 (a) The "ideal" twin polymerization (TP) of **1** to generate a hybrid material consisting of phenolic resin and silica. (b) The introduction of (oligo)-dialkylsiloxane into phenolic resin/silica hybrid materials is possible by simultaneous TP (STP) of **1** with **2**. (c) End-capping of a polyurethane prepolymer with **2** and the subsequent STP results in hybrid materials consisting of phenolic resin, silica and dialkylsiloxane-crosslinked PU.

[a]*Department of Polymer Chemistry, Chemnitz University of Technology, Faculty of Natural Science, D-09107 Chemnitz, Germany. E-mail: katja.schreiter@chemie.tu-chemnitz.de*

[b]*Department of Lightweight Structures and Polymer Technology, Chemnitz University of Technology, Faculty of Mechanical Engineering, D-09107 Chemnitz, Germany*

[c]*BASF Polyurethanes GmbH, Elastogranstraße 60, 49448 Lemfoerde, Germany*

[d]*BASF SE, Carl-Bosch Straße 38, 60756 Ludwigshafen, Germany*

† Electronic supplementary information (ESI) available. See DOI: 10.1039/c8ra05310c

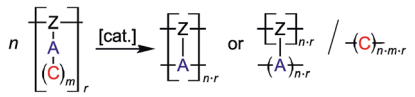

Scheme 2 Twin polymerization of a twin prepolymer.[14]

types of so-called twin monomers (TMs) are suitable for the TP.[16–24] Depending on their molecular structure, two of these monomers can be polymerized simultaneously to generate ternary organic–inorganic HMs (see Scheme 1b).[17,25,26]

Polyurethanes (PUs) are outstanding materials due to their versatility and ability to generate tailor-made properties. The diversity had already been pointed out by O. Bayer in the very first article about PUs.[27] These materials fulfil the varied requirements of modern applications as form-memory polymers, adhesives, foams, fibers, thermoplastic elastomers and coatings.[28–30] As mentioned before, fabrication of nanocomposites or HMs consisting of silica species enables the improvement of material properties like tensile strength or flame retardancy.[9,31] By combining the versatile world of PU chemistry with that of nanostructured HMs accessible by TP, such multicomponent HMs can become accessible. The objective of this work is to present a new concept for combining PU chemistry with that of organic–inorganic HM chemistry.

We describe here the first synthesis of nanostructured phenolic resin/urethane/SiO_2 HMs by simultaneous twin polymerization (STP) using a novel type of urethane-based twin prepolymer and **1**. A urethane-based twin prepolymer is a macromolecule or an oligomer molecule, which can be incorporated into the TP by means of its reactive groups. The synthesis of such twin prepolymers is a subtask of this work. They can be synthesized by use of an amino functionalized TM with isocyanate terminated prepolymer (Scheme 1c).

In the course of the (simultaneous) TP process various scenarios are possible for the formation of the molecular structure of the resulting polymer networks. The inorganic polymer $(A)_n$ can be obtained by reaction with reactive parts from the same or another polymer strand $[Z]_r$ or by a combination of both of these groups (Scheme 2).

Advantageously, the TP process of TM species with benzodioxasiline increments as reactive organic moiety can be induced thermally or by the use of acids or bases as catalyst.[13,14,16,18] In this work, the polymerizations of the considered twin prepolymer systems will be thermally induced and triggered by the use of diazabicyclo[2.2.2]octane (DABCO), or diazabicyclo[5.4.0]undec-7-ene (DBU) as base catalyst, respectively. The polymerization process is carried out in the melt, which is advantageous for possible applications as an adhesion promoter.

Experimental

Materials and methods

Diphenylmethane-4,4′-diisocyanate (MDI), polytetramethylene ether glycole (PTMEG, average molar weight 1000 g mol^{-1}), polypropylene ether glycole (PPG, average molar weight 1000 g mol^{-1}) and PTMEG-MDI-prepolymer (1500 g mol^{-1}) was provided by the BASF SE.

Salicylic alcohol (ABCR), 3-aminopropyl-dimethoxymethylsilane (TCI), tetra-*N*-butylammonium fluoride (1 M solution; ABCR), diazabicyclo[2.2.2]octane (DABCO) (Sigma Aldrich), diazabicyclo [5.4.0]-undec-7-ene (DBU) (fluorochem) were used as received.

All solvents were dried with appropriate drying agents and freshly distilled before usage.

Liquid state ^{1}H NMR (250.1 MHz), ^{13}C NMR (62.9 MHz) and ^{29}Si NMR (49.7 MHz) spectra were recorded with a Bruker DRX 250 NMR spectrometer. The residual signal of the solvent $CDCl_3$ was used as an internal standard relative to tetramethylsilane (TMS; $\delta = 0$ ppm). The ^{29}Si NMR spectra are referenced to TMS ($\delta = 0$ ppm).

Solid state NMR spectra were collected at 9.4 T on a Bruker Avance 400 spectrometer equipped with double tuned probes capable of MAS (magic angle spinning). ^{13}C-{^{1}H}-CP-MAS NMR spectra were measured at 100.6 MHz in 3.2 mm standard zirconium oxide rotors (BRUKER) spinning at 15 kHz. Cross polarization with a contact time of 3 ms was used to enhance the sensitivity. The recycle delay was 6 s. Spectra were referenced externally to tetramethylsilane (TMS) as well as to adamantane as secondary standard (38.48 ppm for ^{13}C). ^{29}Si-{^{1}H}-CP-MAS NMR spectroscopy was performed at 79.5 MHz using 3.2 mm rotors spinning at 12 kHz. The contact time was 3 ms and the recycle delay 6 s. Shifts were referenced externally to tetramethylsilane (0 ppm) with the secondary standard being tetrakis(trimethylsilyl)silane (−9.5 ppm). All spectra were collected with ^{1}H decoupling using a TPPM pulse sequence.

The high annular dark field (HAADF) scanning transmission electron microscopy (STEM) images were recorded with a Technai G2-F-20ST with HAADF-STEM-detector. The samples were prepared by ultramicrotomy.

Electron microscopy images were taken by using an instrument from type Nova NanoSEM 200 of FEI Company after sputtering with platinum.

The DSC measurements were performed by a DSC 1 (Mettler Toledo) and a DSC 204 F1 Phoenix (Netzsch) in a 40 μL aluminum pan and a N_2-flow of 50 mL min^{-1} in a temperature range of 30–300 °C or 30–350 °C with a heating rate of 10 K min^{-1}. The highest and the lowest temperature was held for 3 minutes, respectively.

TGA measurements were performed by a Thermogravimetric Analyzer 7. The samples were measured under air atmosphere, with a heating rate of 10 K min^{-1} from 30–900 °C.

The TG/MS measurements were performed by a TG 209 F1 Iris (Netzsch) coupled to a Aëolos mass spectrometer (Bruker). The samples were prepared in a 85 μL aluminum pan and measured under He-flow of 25 mL min^{-1} in a temperature range of 25–350 °C with a heating rate of 10 K min^{-1}. Before the start of the measurement, the sample room with sample was subjected twice to an evacuation and rinsing cycle with helium.

Size exclusion chromatography (SEC) was performed with a PL-GPC 50 plus from Polymer Laboratories equipped with a PL-AS RT auto sampler and a PC-RI detector. THF was used as eluent with a flow rate of 1.0 mL min^{-1} at 40 °C. The column was a PLgel MIXED-D.

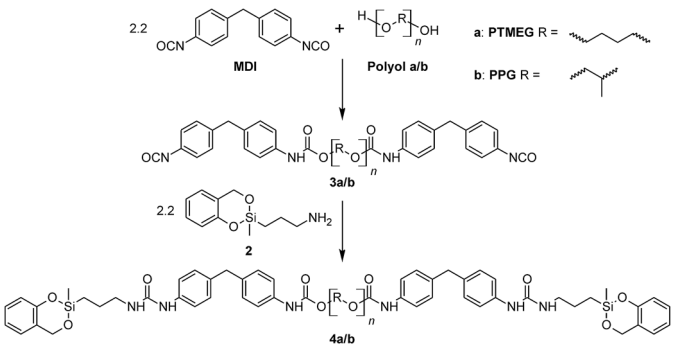

Scheme 3 General procedure for preparation of the twin prepolymer **4a** and **4b**.

The ATR-FTIR-spectra were recorded with a FTS 165 spectrometer (BioRad). A Golden Gate-single reflection-ATR-stage (L.O.T. Oriel GmbH) was used. The samples were pressed against the detection system with a sapphire stamp (5 bar).

Elemental analysis was determined with a Vario El analyser (Elementar analysensysteme GmbH).

Synthetic procedures

Synthesis of the monomers. The synthesis of 2,2′spirobi-[4*H*-1,3,2-benzodioxasiline] (**1**) and 2-(3-aminopropyl)-2-methyl-4*H*-1,3,2-benzodioxasiline (**2**) was already described in the literature and performed accordingly.[12,17]

Procedure for the preparation of 3a/b (spectral data can be found in the ESI†). 2.2 equivalents MDI were heated to 50 °C. One equivalent PTMEG (for **3a**) or PPG (for **3b**) was added under stirring to the molten diisocyanate by a dropping funnel within 15 minutes. Afterwards, the reaction mixture was heated to 98 °C for 2 h.

General procedure for end-capping of prepolymer in substance. The end-capping was performed subsequently to the prepolymer preparation. Under stirring, 2.2 equivalents **2** were slowly added with a syringe through a septum to the prepolymer **3a** or **3b** at 70 °C. During the addition of **2** the temperature was kept below 100 °C. The reaction mixture was stirred at 70 °C for 30 minutes to give the products **4a** or **4b**.

Polymerization

General procedure for the thermal induced STP of 4a/b with 1. The respective amounts of **4a/b** and **1** were placed in a PTFE-wide-neck-flask with screw-cap and magnetic stirrer under argon. Under stirring, the flask was heated to 125 °C for 0.5 h to give a homogeneous melt. The magnetic stirrer was removed from the slightly yellow reaction mixture. Afterwards the reaction-flask was heated to the respective polymerization temperature for 2 h.

Detailed information are summarized in the ESI. The monomer amounts, extractable contents as well as the found silicon contents are listed in Tables 2/3.

Extraction

The obtained materials were cut into small pieces with a scalpel. About 1 g of the material pieces were placed in an extraction thimble and Soxhlet-extracted with 200 mL dichloromethane for 48 h. The extracted material was dried in a vacuum oven at 40 °C until weight constant. The solvent was removed under reduced pressure to give the concentrated extract.

Results and discussion

The reactive prepolymers **4a** and **4b** were obtained by end-capping of the PU prepolymers **3a** or **3b** with 2-(3-aminopropyl)-2-methyl-4*H*-1,3,2-benzodioxasiline (**2**), respectively.

In accordance to the classification of TM species and polymerization processes, a so-called twin prepolymer was generated (Scheme 3).[14]

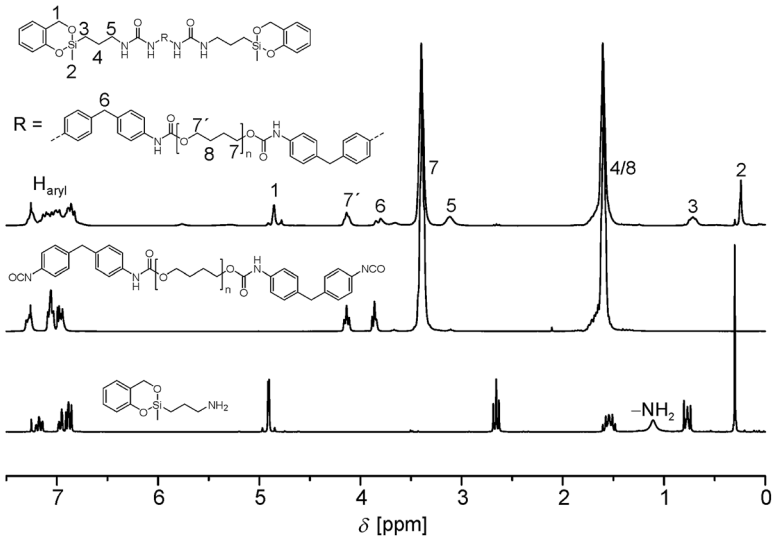

Fig. 1 ^{1}H NMR spectrum of **4a** (top) in combination with the spectra of the corresponding educts **2** (bottom) and **3a** (middle, all spectra measured in $CDCl_3$).

A representative ^{1}H NMR spectrum of **4a** is shown in Fig. 1. The disappearance of the NH_2 signal and the down field shift of the neighboring CH_2 group of **2** (signal 5) prove the successful reaction of the amino functionality with isocyanate.

Due to the required excess of diisocyanate used during the preparation of the prepolymer, low molecular by-products can be detected by GPC measurement (Fig. S4/S5 and Tables S1/S2†). Those by-products have to be taken into account for the subsequent polymerization and its interpretation.

Thermal initiation – preliminary investigation

Polymerization ability of the twin prepolymers **4a** and **4b** were studied using differential scanning calorimetry (DSC). Various reaction scenarios are apparent from the temperature profiles, showing the reaction of a twin prepolymer alone, in the presence of a second TM or with a potential catalyst (Fig. 2). Homogenous monomer mixtures were prepared by melting all components at 100 °C prior to the DSC measurements.

Upon heating the twin prepolymer **4a**, an exothermic peak at 279 °C (T_{onset} = 234 °C, Fig. 2 bottom) is observed. The addition of **1** reduces the trigger temperature as indicated by the exothermic peak to 245 °C (T_{onset} = 150 °C, Fig. 2 middle). If DABCO is added as a catalyst to that mixture a further reduction of the polymerization trigger temperature (Fig. 2 top) is measured. Two exothermic peaks (T_{onset1} = 117 °C, T_{peak1} = 142 °C; T_{onset2} = 195 °C, T_{peak2} = 229 °C) are obtained, the first one indicating its catalytic activity.

The addition of lactic acid as catalyst to the mixture of **4a** and **1** already leads to polymerization at a temperature of approx. 80 °C. However, a prerequisite for a polymerization in the melt of **4a** and **1** is a mixing of the components at approx. 100 °C. Otherwise, inhomogeneous products are created due to the high viscosity of the reaction mixture. Therefore, acid catalysis was not preferred in this work, although this problem can be solved by using a solvent but that is not useful for the objective of this work.

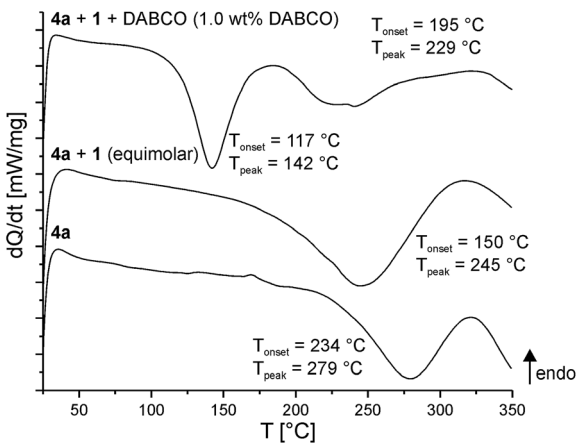

Fig. 2 DSC curves of the twin prepolymer **4a** alone, with equimolar amounts of **1** and an equimolar mixture of **4a** and **1** with 1.0 wt% of base catalyst (DABCO); heating rate 10 K min^{-1}.

Table 1 Characteristic trigger temperatures for thermally induced and DABCO catalyzed STP of different monomer mixtures of **4a** or **4b** with **1** as determined by DSC measurements

	$T_{onset,exo}$ ($T_{peak,exo}$) [°C]	
	4a	**4b**
Pure	234 (279)	245 (293)
+**1**	150 (245)	191 (237)
+**1** + DABCO	117 (142)	134 (148)
	195 (229)	

4b alone shows an exothermic peak at 293 °C. The addition of **1** and DABCO results in similar trends to lower temperatures as observed for **4a** (Table 1 and Fig. S12†).

These preliminary results were confirmed by reproducing these polymerizations on a multi-gram scale and subsequent analysis of the products. Monolithic HMs were prepared by thermal polymerization, with the addition of either DABCO or DBU as catalysts.

Thermally induced (simultaneous) twin polymerization

The prepolymers **4a** or **4b** were polymerized simultaneously with **1** at 170 °C, 190 °C, 210 °C as well as 230 °C for 2 h using a stoichiometric ratio of 1 : 1 (Table 2). The yellow colored materials obtained are readily foamed and elastic. According to the concept of STP, the resulting organic–inorganic HM should consist of phenolic resin, SiO_2 and oligodialkylsiloxane (ODAS) with integrated urethane structural units which also have a cross-linking function. The SiO_2 and ODAS groups can form Si–O–Si bonds and thus form a class II hybrid structure among the phenolic resin/SiO_2/ODAS hybrid compounds according to the classification of Sanchez[32] (Scheme 4). This is verified by ^{29}Si and ^{13}C solid state NMR spectroscopy of the HMs (Fig. S6†).

Each of the ^{29}Si-{^{1}H}-CP-MAS NMR spectrum of HMs show the expected Q and D signals resulting from monomer **1** and the corresponding twin prepolymer, respectively. The Q_4 signals measured at −110 ppm are the most intense signals in the silica range (= Q) of the ^{29}Si NMR spectrum in each case. The cross polarization technique used to enhance the sensitivity

Table 2 Summary of the synthesis conditions of the hybrid materials and the composition as measured by thermogravimetric analysis (TGA) after extraction. Reaction time t = 2 h. Calculated silica content = 8.1 wt%

Sample	Molar ratio [mol%] $n_{\mathbf{4a/b}} : n_{\mathbf{1}}$	Temp. [°C]	Extr. cont. [wt%]	Silica cont. [wt%]
HM5a_170	50 : 50	170	47	10.7
HM5a_190		190	47	11.1
HM5a_210		210	35	9.2
HM5a_230		230	36	10.5
HM5b_170	50 : 50	170	84	—
HM5b_190		190	49	11.1
HM5b_210		210	33	11.5
HM5b_230		230	45	9.2

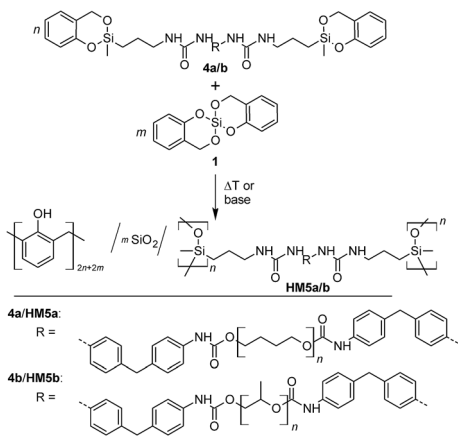

Scheme 4 Reaction scheme for the STP of **4a/b** with **1**.

overestimates Q_2 (−90 ppm) and Q_3 (−100 ppm) over Q_4 because these are silicon species with hydrogen in close proximity resulting in a more efficient polarization transfer from ^1H to ^{29}Si. The high intensity of the Q_4 signals in comparison to Q_2 and Q_3 found in the products clearly shows that the SiO_2 network must nearly be fully condensed.

The D_1, D(Q) and D_2 signals observed in the range from −10 to −23 ppm correspond to bifunctional (D) silicon structures originating from **4a**, or **4b**. D(Q) signals are also found at about −16 to −17 ppm. These are characteristic for the STP products indicating a reduced flexibility of the oligodialkylsiloxane (ODAS) part and thus the binding of ODAS to the SiO_2 network. According to the classification of STP processes,[25] this is therefore a real simultaneous twin copolymerization. The observation of a D_1 (one siloxane bond, Si–O–Si–) signal at ≈−7 ppm probably corresponds to end groups of ODAS. No signals from the monomer reactants were detected in the solid state ^{29}Si NMR spectra.

The formation of phenolic resin, ODAS and urethane structures can be proven by ^{13}C-{^1H}-CP-MAS NMR spectroscopy. The *o*,*o*′- and *o*,*p*′-bonded phenolic resin structures can be detected by the signals in the aromatic region (signals 3 and 5, Fig. S6†). The signal for the bridging methylene group (signal 4) is overlaid with the intense signal of the CH_2 groups of the ether fragment (signal 15). The ODAS structure gives a signal for the methyl group at 0 ppm. The signals for the carbon atoms of the alkyl chains of ODAS are observed in the expected region of 18–70 ppm, whereby the most intense carbon signals at 26 and 70 ppm are due to the methylene groups of the ether fragments (signals 14 and 15). Furthermore, the presence of signals at 42 ppm (signal 11), between 110–140 ppm (signal 12) and 155 ppm (signal 10 and 13), shows that the urethane fragment is bonded to HM after the polymerization and subsequent extraction.

Soxhlet-extraction of the raw HM with dichloromethane (DCM) gave extractable fractions, which were identified as prepolymer and low molecular weight products such as salicylic alcohol (Fig. S7 and Table S7†). Depending on the polymer backbone chosen, the quantity of the extractable fraction was very different. Using **4a** gives an extractable portion of 47 wt% whereas with **4b** the extractable portion increases to 84 wt%. These extraction experiments together with the results of the DSC (Fig. S12†) show that for the system **4b : 1** a polymerization temperature of 170 °C is too low (Table 2).

Thus, the HMs of the monomers **1** and **4a** or **4b** were polymerized at higher temperatures (190 °C/210 °C/230 °C) to increase the conversion.

Increasing the polymerization temperature to 210 °C results in a reduction of the extractable proportions of the resulting HMs to ≈35 wt% for **4a** and ≈33 wt% for **4b** (T = 210 °C, $n_{4a/b} : n_1 = 1 : 1$) (Table 2). Subsequent DSC measurements do not show any subsequent reactions during the thermal treatment of the materials (Fig. S13†). The large amount of extractable portions can, on the one hand, be attributed to this sterically demanding prepolymer, on the other hand because the polymerization process is a bulk polymerization, *i.e.* the increasing viscosity during polymerization is a limiting factor for complete conversion. At a temperature of 230 °C highly foamed partly dark-colored HMs were obtained. TG-MS measurements show that during the polymerization process CO_2 and traces of water are liberated (Fig. S17†). Urethane and urea increments are, after biuret and allophanate substructures, the most thermally labile compounds in a PU formulation.[33–35] In order to reduce the thermal load on the samples and thus avoid dissociation of the urethane bonds, only the twin prepolymer **4a** was selected for further experiments involving variation of the monomer ratios at a polymerization temperature of 170 °C. Varying the monomer ratio of **4a : 1** gives no clear trend with regard to the amount of extractable material (Table 3). NMR spectras of the extract showed again prepolymer residues and low molecular weight products such as salicylic alcohol (Fig. S8 and Table S8†).

Solid-state ^{13}C and ^{29}Si NMR spectroscopy proves the formation of the phenolic resin, silica and ODAS (Fig. 3). The different monomer ratios of **4a : 1** are reflected in the NMR spectra and the signal intensities of phenolic resin/ODAS varies correspondingly. An increasing content of the monomer **4a** leads to formation of more ODAS structures and thus to more intense D signals, as are shown in the ^{29}Si NMR spectra (Fig. 3). A lower monomer **4a** ratio gives a strong signal at −17 ppm, which represents D(Q) species. As expected, **HM5a**_100 shows only D and no Q signals because of the absence of **1** as reactant.

The signals of the phenolic carbon and the urethane carbon atom have quite similar chemical shifts within ^{13}C solid state NMR spectra and cannot be distinguished due to broad line widths. The ^{13}C NMR signals in the chemical shift range of 110

Table 3 Summary of experiments performed with different molar ratios of monomers (*n*) and composition as measured by TGA after extraction. Reaction conditions: t = 2 h, T = 170 °C

Sample	Monomer ratio $n_{4a} : n_1$ [mol%]	Extr. cont. [wt%]	Silica cont. [wt%] (TGA)	Silica cont. [wt%] (calc.)
HM5a_05	5 : 95	21	20.9	17.6
HM5a_15	15 : 85	33	18.7	13.0
HM5a_50	50 : 50	47	10.7	8.1
HM5a_85	85 : 15	25	6.1	6.5
HM5a_100	100 : 0	14	5.7	6.2

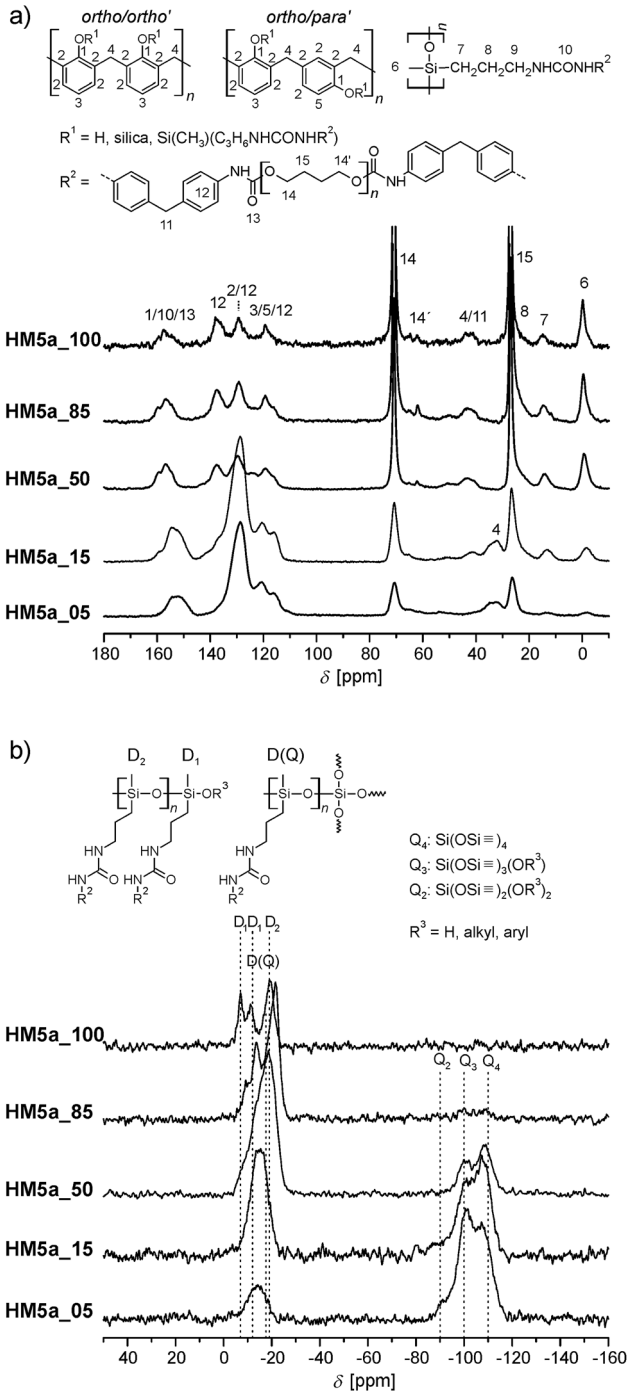

Fig. 3 Solid-state-NMR spectra of selected samples with different molar ratios of the monomers **4a** and **1**. (a) ^{13}C-{^{1}H}-CP-MAS@15 kHz (number of scans: **5a**_100 14190; **5a**_85 39776; **5a**_50 14077; **5a**_15 47345; **5a**_05 15476) (b) ^{29}Si-{^{1}H}-CP-MAS@12 kHz (number of scans: **5a**_100 14184; **5a**_85 45596; **5a**_50 62126; **5a**_15 15012; **5a**_05 14716).

to 140 ppm can be assigned to aromatic carbons. The phenolic resin as well as the used aromatic isocyanate contains such structures. Thus, it cannot be determined with certainty whether phenolic resin is formed in the homo polymerization of prepolymer **4a** ($n_{\mathbf{4a}} : n_{\mathbf{1}} = 100 : 0$). In order to determine whether the twin prepolymer participates in the polymerization reaction under formation of phenolic resin a third twin prepolymer **4c** was synthesized using the aliphatic diisocyanate IPDI (Scheme 5; ESI†). In the absence of aromatic carbon atoms in the isocyanate component it is possible to determine unequivocally whether phenolic resin is being formed during the homo-polymerization of the twin prepolymer by ^{13}C NMR spectroscopy. The spectra of **4c** (in $CDCl_3$) and that of its corresponding homo-polymer **HM5c**_100 are shown in Fig. 4. After the polymerization (170 °C, 2 h) and extraction of the HM, characteristic signals in the range 110–133 ppm are seen, demonstrating the formation of phenolic resin even in the absence of co-monomer **1**.

As shown in Fig. 3(a), the characteristic ^{13}C signals of the urethane bond and the phenolic resin cannot be identified separately from each other (signals 1, 9 and 12 in Fig. 3). ^{29}Si-{^{1}H}-CP-MAS NMR spectroscopy is used to show the successful polymerization of the dialkyl siloxane increments of the TM end groups (Fig. 3).

In order to test whether the urea increment is present after the polymerization, the HM was investigated by ATR-FT-IR spectroscopy. The materials **HM5a**-100/85/50/15/5 as well as **4a** show, in comparison with prepolymer **3a**, an additional band at 1642 cm^{-1} assigned to the stretching vibration of the C═O$_{urea}$ group. In prepolymer **3a** this band is, as expected, not detectable (Fig. S18†).

All HM were investigated by thermogravimetric analysis (TGA). The samples were heated to 900 °C under air atmosphere with a heating rate of at 10 K min^{-1} and held for 10 minutes at this temperature in order to guarantee complete removal of the organic content. The quantity of the residue reflects the amount of inorganic material introduced in the HM by variation of the monomers used in each experiment. The thermogravimetric analysis (TGA) of the organic–inorganic HMs shows a slight loss in weight of 4.8 wt% (**HM5a**_15) to 9.6 wt% (**HM5a**_85) between 30 and 300 °C.

Base catalyzed simultaneous twin polymerization

Thermally initiated STP of **4a** and **1** fabricates to a phenolic resin/SiO_2/ODAS nanocomposite in a single step. However, the TP can also be catalyzed by acids or bases. The addition of acid (*e.g.* lactic acid) to a mixture of **4a** and **1** reduces the

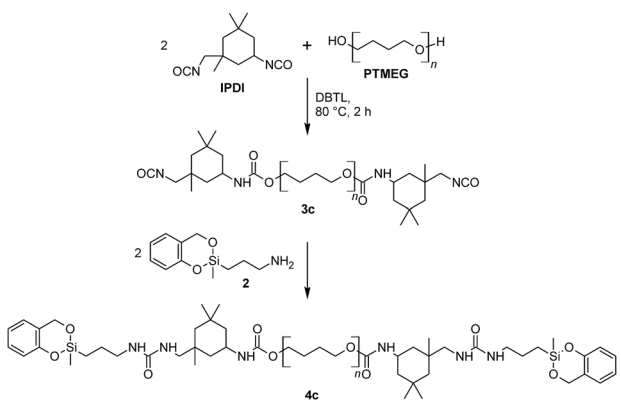

Scheme 5 Preparation of the aliphatic prepolymer **3c** with DBTL-catalyst and the end-capping with **2** to obtain **4c**.

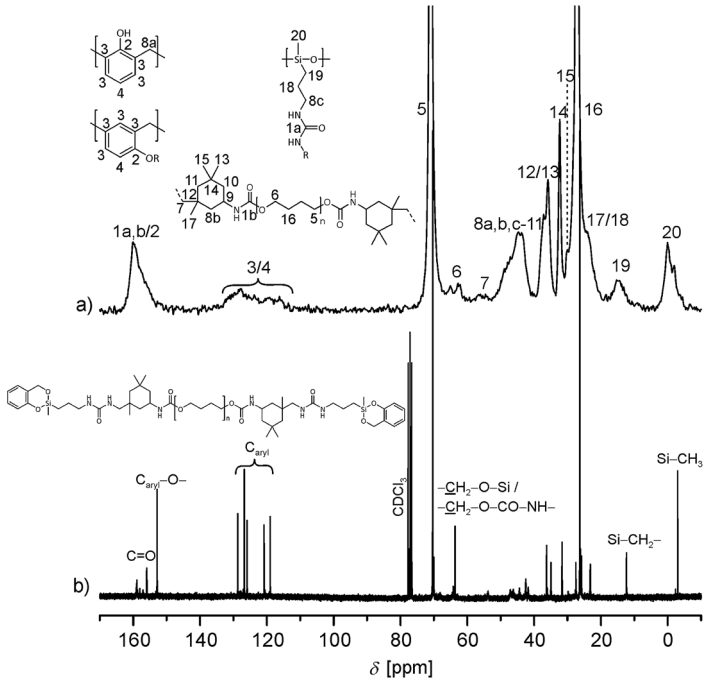

Fig. 4 (a) ^{13}C-{^{1}H}-CP-MAS spectrum of the extracted polymer **HM5c**_100 prepared by the thermally induced polymerization of **4c**. (b) Liquid-state NMR of **4c** (in $CDCl_3$).

polymerization temperatures to 80 °C. Unfortunately, the high viscosity results in poor mixing and lead to heterogeneous products. In comparison, the base-catalyzed polymerization of **4a** and **1** requires activation temperatures higher than 120 °C as concluded from DSC measurements (see Fig. 2). Thus, the necessary polymerization temperature lies between those of the thermally induced and the acid-catalyzed polymerizations. 1,4-diazabicyclo[2.2.2]octane (DABCO) and 1,8-diazabicyclo[5.4.0] undec-7-ene (DBU) were used as base catalysts. A selection of the experiments performed is shown in Table 4.

The base-catalyzed STP results in clearly lower extractable portions compared with the thermally induced TP despite the lower reaction temperatures. The soluble extracts show the same composition as for the HM produced by thermal initiation without base as catalyst (Fig. S11†).

High angle annular dark field scanning transmission electron microscopy (HAADF-STEM) investigations were carried out to achieve information on the sizes of the phase domains of the HMs obtained. This technique shows an elemental contrast as well as the contrast attributed to the thickness and the density of the sample. With increasing atomic weight, a higher signal intensity is observed. Thus, the silicon-rich domains of the HM are brighter than the organic polymer. The HAADF-STEM pictures of selected samples with different monomer compositions of **4a** and **1** show bright SiO_2 clusters with a size of about 2 nm. However, the monomer compositions chosen do not have a significant effect on the domain size (Fig. 5). Si-rich domains are clearly smaller than those found in comparable phenolic resin-silicon dioxide composite materials which were synthesized *via* sol–gel process.[36,37]

Fig. 6 shows HAADF-STEM pictures of HMs produced from thermally induced and base catalyzed (DABCO) STP of **4a** and **1** in equimolar ratio. The silicon distribution within **HM5a**_base_2 is slightly more homogeneous compared with **HM5a**_50. STPs of both pre-polymers, **4a** and **4b**, respectively, in combination with **1** result in HMs which show a quite similar structure in the high resolution TEM pictures: bright SiO_2 clusters with a size of approximately 2 nm (**HM5a**_50 polymerized at 170 °C, **HM5b**_190

Table 4 Summary of the synthesis conditions of the hybrid materials (*via* base catalyzed STP) and the composition as measured be thermogravimetric analysis (TGA) after extraction. Reaction time $t = 2$ h. Calculated silica content = 8.1 wt%

Sample	Catalyst (base)	Conc. (base) [mol%]	T [°C]	Extr. cont. [wt%]	Silica cont. [wt%]
4a and 1					
HM5a_base_1	DABCO	2.3	120	18	8.3
HM5a_base_2		9.0	120	17	9.6
HM5a_base_3			140	19	9.6
HM5a_base_4	DBU	6.0	150	18	9.0
4b and 1					
HM5b_base_1	DABCO	6.0	140	15	8.7

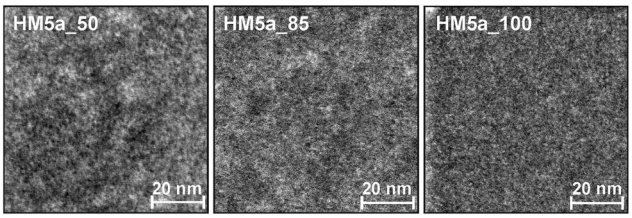

Fig. 5 HAADF-STEM-images of hybrid materials with different monomer ratios of **4a** and **1**.

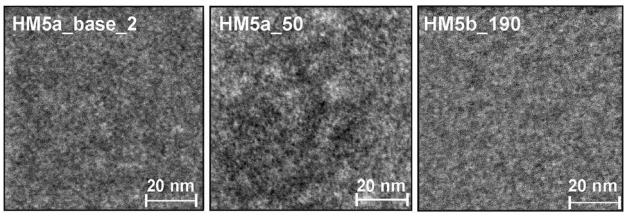

Fig. 6 HAADF-STEM images of the HM prepared by the STP of **4a** and **1** with the use of a base catalyst (**HM5a**_base_2, DABCO, 9.0 mol%/1 wt%, 120 °C, 2 h), the HM prepared by thermally induced STP of **4a** and **1** (**HM5a**_50, equimolar, 170 °C, 2 h) and the HM prepared by thermally induced STP of **4b** and **1** (**HM5b**_190, equimolar, 190 °C, 2 h).

polymerized at 190 °C, Fig. 6). The monomer ratios chosen have no significant effect on the size of the phase domains.

Conclusions

Novel twin prepolymers **4a–c** were synthesized and their polymerization ability to produce nanostructured HMs was demonstrated. It was shown that the choice of polymer backbone in the twin prepolymers has an effect on the necessary trigger temperature of the TP. Organic–inorganic HMs are accessible by means of the synergistic combination of twin prepolymers **4a**/**b** with 2,2′-spirobi[4*H*-1,3,2-benzo-dioxasiline] (**1**) using STP. The interpenetrating networks resulting from three different polymers result in nanostructured phase domains of approximately 2–4 nm in size. The different networks are formed on the same time scale. Therefore the phase separation is very small and very similar to the already known hybrid materials from twin polymerization. This represents a completely new procedure for incorporating various types of silicon and phenolic resin into nanoscale urethane formulations. The careful choice of monomer composition and trigger process for polymerization procedure is key for the material properties of the HM produced. A correlation of the molecular structure of the organic–inorganic HM with urethane increments with their macroscopic properties is important for the construction of nanocomposites with specific properties required for industrial applications, *e.g.* construction of strongly adhering, flexible interlayers in lightweight structures, which is the aim of future work.

Conflicts of interest

There are no conflicts to declare.

Acknowledgements

We thank the BASF SE for particular financial support, the providing of chemicals as well as the measurement of the HAADF-STEM-images. This work was also supported by the Deutsche Forschungsgemeindschaft (SCHR 1469/1-1 and the Federal Cluster of Excellence EXC 1075 "Technology Fusion for Multifunctional Lightweight Structures"). Furthermore, we acknowledge Prof. Hietschold and Prof. Tegenkamp for the opportunity of measuring electron microscopy images.

Notes and references

1 M. Christopher Orilall and U. Wiesner, *Chem. Soc. Rev.*, 2011, **40**, 520–535.
2 M. Antonietti, *Sci. Bull.*, 2016, **61**, 1662–1664.
3 A.-H. Lu, W.-C. Li, G.-P. Hao, B. Spliethoff, H.-J. Bongard, B. B. Schaack and F. Schüth, *Angew. Chem., Int. Ed.*, 2010, **49**, 1615–1618.
4 Y. Yamauchi, N. Suzuki, L. Radhakrishnan and L. Wang, *Chem. Rec.*, 2009, **9**, 321–339.
5 M. Antonietti, *Nat. Mater.*, 2003, **2**, 9.
6 A. S. Aricò, P. Bruce, B. Scrosati, J.-M. Tarascon and W. van Schalkwijk, *Nat. Mater.*, 2005, **4**, 366.
7 A. Thomas, F. Goettmann and M. Antonietti, *Chem. Mater.*, 2008, **20**, 738–755.
8 H. S. Thiam, W. R. W. Daud, S. K. Kamarudin, A. B. Mohammad, A. A. H. Kadhum, K. S. Loh and E. H. Majlan, *Int. J. Hydrogen Energy*, 2011, **36**, 3187–3205.
9 Y. Chen, S. Zhou, H. Yang and L. Wu, *J. Appl. Polym. Sci.*, 2005, **95**, 1032–1039.
10 S. Karataş, Z. Hoşgör, N. Kayaman-Apohan and A. Güngör, *Prog. Org. Coat.*, 2009, **65**, 49–55.
11 S. Karataş, Z. Hoşgör, N.-K. Apohan and A. Güngör, *J. Polym. Res.*, 2010, **17**, 247–254.
12 S. Spange, P. Kempe, A. Seifert, A. A. Auer, P. Ecorchard, H. Lang, M. Falke, M. Hietschold, A. Pohlers, W. Hoyer, G. Cox, E. Kockrick and S. Kaskel, *Angew. Chem., Int. Ed.*, 2009, **48**, 8254–8258.
13 P. Kempe, T. Löschner, A. A. Auer, A. Seifert, G. Cox and S. Spange, *Chem. – Eur. J.*, 2014, **20**, 8040–8053.
14 T. Ebert, A. Seifert and S. Spange, *Macromol. Rapid Commun.*, 2015, **36**, 1623–1639.
15 P. Kitschke, A. A. Auer, T. Löschner, A. Seifert, S. Spange, T. Rüffer, H. Lang and M. Mehring, *ChemPlusChem*, 2014, **79**, 1009–1023.
16 S. Spange and S. Grund, *Adv. Mater.*, 2009, **21**, 2111–2116.
17 M. Göring, A. Seifert, K. Schreiter, P. Müller and S. Spange, *Chem. Commun.*, 2014, **50**, 9753–9756.
18 A. Mehner, A. Pohlers, W. Hoyer, G. Cox and S. Spange, *Macromol. Chem. Phys.*, 2013, **214**, 1000–1010.
19 S. Oschatz, A. Lange, S. Csihony, G. Cox, O. Gronwald, A. Seifert and S. Spange, *J. Polym. Sci., Part A: Polym. Chem.*, 2016, **54**, 2312–2320.
20 C. Leonhardt, A. Seifert, S. Csihony, H. Sommer and M. Mehring, *RSC Adv.*, 2016, **6**, 3091–3098.

21 L. Kaßner, K. Nagel, R.-E. Grützner, M. Korb, T. Rüffer, H. Lang and S. Spange, *Polym. Chem.*, 2015, **6**, 6297–6304.
22 P. Kitschke, M. Walter, T. Rüffer, A. Seifert, F. Speck, T. Seyller, S. Spange, H. Lang, A. A. Auer, M. V. Kovalenko and M. Mehring, *J. Mater. Chem. A*, 2016, **4**, 2705–2719.
23 F. Böttger-Hiller, A. Mehner, S. Anders, L. Kroll, G. Cox, F. Simon and S. Spange, *Chem. Commun.*, 2012, **48**, 10568–10570.
24 A. Mehner, T. Rüffer, H. Lang, A. Pohlers, W. Hoyer and S. Spange, *Adv. Mater.*, 2008, **20**, 4113–4117.
25 T. Löschner, A. Mehner, S. Grund, A. Seifert, A. Pohlers, A. Lange, G. Cox, H.-J. Hähnle and S. Spange, *Angew. Chem.*, 2012, **124**, 3312–3315.
26 J. Weißhuhn, T. Mark, M. Martin, P. Müller, A. Seifert and S. Spange, *Polym. Chem.*, 2016, **7**, 5060–5068.
27 O. Bayer, *Angew. Chem.*, 1947, **59**, 257–272.
28 H.-W. Engels, H.-G. Pirkl, R. Albers, R. W. Albach, J. Krause, A. Hoffmann, H. Casselmann and J. Dormish, *Angew. Chem., Int. Ed.*, 2013, **52**, 9422–9441.
29 N. Adam, G. Avar, H. Blankenheim, W. Friederichs, M. Giersig, E. Weigand, M. Halfmann, F.-W. Wittbecker, D.-R. Larimer, U. Maier, S. Meyer-Ahrens, K.-L. Noble and H.-G. Wussow, in *Ullmann's Encyclopedia of Industrial Chemistry*, Wiley-VCH Verlag GmbH & Co. KGaA, 2000.
30 U. Meier-Westhues, *Polyurethane – Lacke, Kleb- und Dichtstoffe*, Vincentz Network GmbH & Co. KG, Hannover, 2007.
31 H. Zou, S. Wu and J. Shen, *Chem. Rev.*, 2008, **108**, 3893–3957.
32 C. Sanchez and F. Ribot, *New J. Chem.*, 1994, **18**, 1007–1047.
33 M. Ravey and E. M. Pearce, *J. Appl. Polym. Sci.*, 1997, **63**, 47–74.
34 F. E. Rogers and T. J. Ohlemiller, *J. Macromol. Sci., Chem.*, 1981, **15**, 169–185.
35 S. V. Levchik and E. D. Weil, *Polym. Int.*, 2004, **53**, 1585–1610.
36 H. Sardon, L. Irusta, M. J. Fernández-Berridi, M. Lansalot and E. Bourgeat-Lami, *Polymer*, 2010, **51**, 5051–5057.
37 Y. Zhu and D.-X. Sun, *J. Appl. Polym. Sci.*, 2004, **92**, 2013–2016.